CHARACTERISTICS OF A PLASMATRON WITH AN ARC CHAMBER OF VARIABLE RADIUS

A. I. Dautov, R. Kh. Ismagilov,
Kh. M. Shavaliev, and A. G. Shashkov

UDC 533.9.07

Experimental data have been obtained on the thermal and electrical characteristics of a plasmatron with an arc chamber of variable radius. It is shown that the characteristics of the arc chamber can be improved by fabricating the chamber with a particular profile.

Arc chambers of variable cross section are of interest in connection with the development of optimal plasmatrons. It has been shown (see, e.g., [1]) that plasmatrons with a stepped anode channel have several advantages. The use of a section of variable cross section in the anode region of a plasmatron in an effort to shield the cathode from agressive gases also has beneficial effects [2]. Accordingly, it is pertinent to study plasmatrons with arc chambers of variable cross section.

We report here an experimental study of a plasmatron with an arc chamber of variable radius and with a distributed gas supply. For this plasmatron the channel radius varies according to $R = R_0\sqrt{1+kz}$, and there is a distributed supply of the gas through the intersectional gaps of the arc chamber (Fig. 1). In these experiments the flow rate $G_i = G_0(k/L)(l+\delta)$ is held at such a level that the mass flow rate $\rho v = G/\pi R^2$ is constant along the length of the chamber. This type of gas supply was chosen so that the experimental data could be compared with the results of [3], where a theoretical study was made of the properties of the positive column of an arc under the assumption of a constant product ρv. The experiments were carried out over the ranges $G_i = (1\text{-}4) \cdot 10^{-3}$ kg/sec and I = 100-400 A with $R_1 = 0.75 \cdot 10^{-2}$ m, L = 0.18 m, $l = 0.016$ m, $\delta = 0.2 \cdot 10^{-2}$ m, $l_a = 0.025$ m, and atmospheric pressure at the exit from the plasmatron.

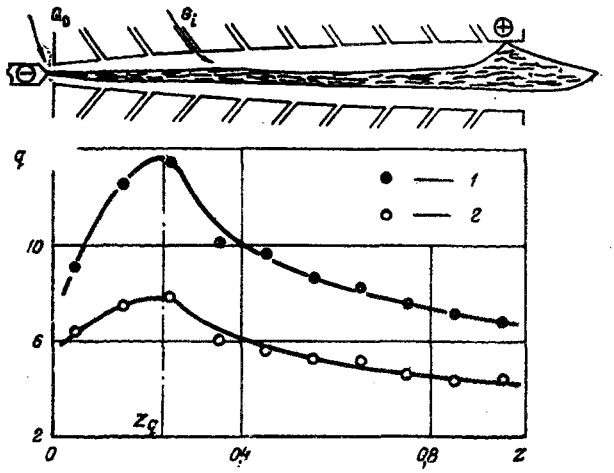

Fig. 1. Distribution of the heat flux $q \cdot 10^{-4}$ along an arc chamber for $G_0 = 0.317 \cdot 10^{-3}$ kg/sec, $G_i = 0.166 \cdot 10^{-3}$ kg/sec, and k = 5.25. 1) I = 200; 2) 150. Shown at the top is a diagram of the arc chamber of the plasmatron. Here q is expressed in W/m.

Kazan' Institute of Aviation. Translated from Inzhenerno-Fizicheskii Zhurnal, Vol. 28, No. 5, pp. 860-865, May, 1975. Original article submitted October 21, 1974.

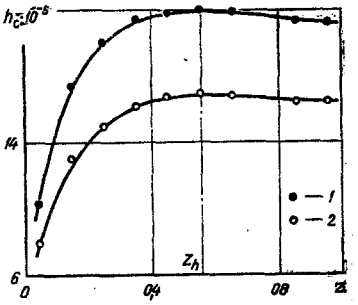

Fig. 2

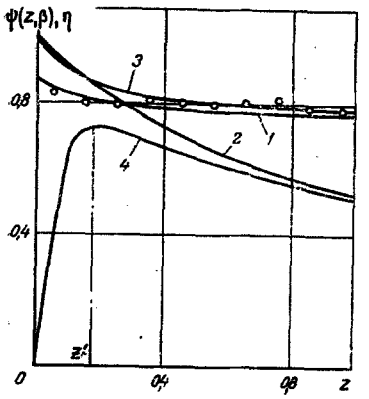

Fig. 3

Fig. 2. Profile of the average-mass enthalpy along the arc chamber. 1) I=200; 2) 150. $G_0 = 0.317 \cdot 10^{-3}$ kg/sec, $G_i = 0.166 \cdot 10^{-3}$ kg/sec^{-1}, k=5.25. Here h_c is expressed in J/Kg.

Fig. 3. Distributions of η (curves 1, 3, and the points) and $\psi(z, \beta)$ (curves 2 and 4) along a positive column for k=5.25 and $\beta = 12$. 1, 2) Calculated for $E_0 = E_0'$; 3, 4) calculated for $E_0 = \infty$; points) experimental values of η for I=110 *a*.

In a channel of constant radius with a flowing gas the properties of the arc reach their limiting values very rapidly, and the electric field, the temperature, and the heat flux are constant along the length of the channel [4, 5]. Figure 1 shows that under these conditions the distribution of q is qualitatively different from that described above: At the beginning of the channel, it increases along the z axis, reaches a maximum in cross section Z_q, and then falls off monotonically with a further increase in the channel radius. The position Z_q depends on the geometry of the channel and the section, the gas flow rate, the current, and several other factors. It turned out, however, that over the ranges of parameters studied, the value of Z_q is governed primarily by G_0, so that in calculating Z_q we can use the approximate equation

$$Z_q = cLG_0, \; c = 665 \frac{\text{sec}}{\text{kg}}, \tag{1}$$

obtained in an analysis of the experimental data.

The h_c distribution is analogous to the q distribution, but the maximum of h_c is not as prominent, and at small currents the value of h_c becomes nearly independent of z at Z_h (Fig. 2). Accordingly, the value of Z_h determines the length of the initial region of the arc, in which the most pronounced changes in the properties of the arc along the z axis occur.

Analysis of the experimental data reveals that, despite the complex q and h_c distributions, the electric field falls off along the entire length of the interelectrode insert. It should be noted that, while this decrease is due to the rapid expansion of the channel and the rapid increase in the temperature in the downstream direction up to cross section Z_h, the further decrease at $z > Z_h$ is due solely to an increase in the radius of the arc chamber. As expected, E increases with increasing G_i, but the form of the E(z) curves

TABLE 1. Dependences of μ_1, γ_1, and Φ_1' on β

β	μ_1	γ_1	$-\Phi_1'$
0	2,4048	0,2159	1,2484
2	2,6149	0,1995	0,9653
4	2,8284	0,1839	0,7357
6	3,0443	0,1692	0,5529
8	3,2613	0,1554	0,4096
10	3,4783	0,1427	0,2994
12	3,6945	0,1309	0,2159
14	3,9088	0,1203	0,1537
16	4,1204	0,1106	0,1081
18	4,3287	0,1019	0,0752
20	4,5332	0,0941	0,0517

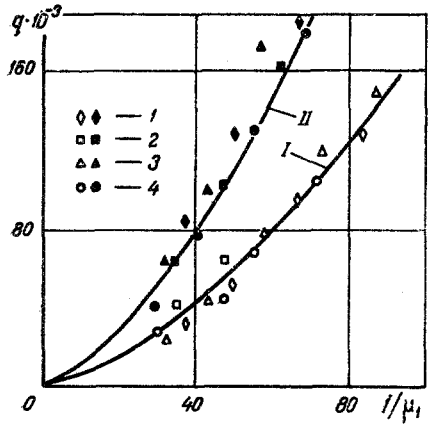

Fig. 4

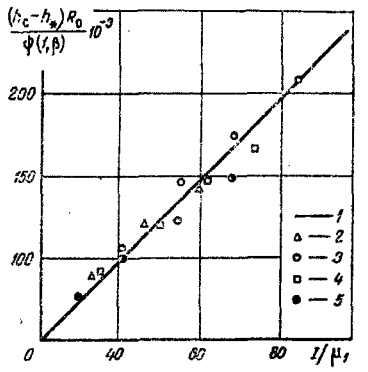

Fig. 5

Fig. 4. Dependence of the heat flux on I/μ_1 at $z=1$ (curve I) and $z=Z_m$ (II). $k=5.25$. 1) $\beta=6$; 2) 8; 3) 10; 4) 12. Here q is expressed in w/m and I/μ_1 is expressed in A.

Fig. 5. Generalized dependence of the relative enthalpy. 1) Calculated; 2-4) $k=3.1$; 2) $\beta=10$; 3) $\beta=12$; 4) $\beta=16$; 5) $k=5.25$, $\beta=12$. Here I/μ_1 is expressed in A and $(h_c-h_*)R_0/\psi(1,\beta)$ is expressed in J · m/kg.

remains essentially the same. Over the I range studied we observed no significant effect of I on E or U. This is a typical result for arcs with distributed flow and is due to the strong dependence of the radius of the positive column on the current and the gas flow rate [6].

One way to increase the plasmatron power is to use long interelectrode inserts. However, in a channel with a constant radius and a constant flow rate, there is a limit on the length of the insert because of the z dependence of η and the circumstance that only the initial and transitional parts of the arc are useful from the standpoint of increasing the plasmatron power and efficiency. It has been shown in several studies (e.g., [5, 7]) that when a distributed gas flow is used it becomes possible to maintain quite large values of η even near the end of the arc, but because the extreme parameters are reached rapidly and because of the intense cooling of the positive column it is not possible to greatly raise the average-mass temperature [3, 8]. Experiments have shown that, in this case, the value of η remains constant along the length of the channel, is a weak function of I, and is governed primarily by G_l. Because of the progressive increase in the channel radius, the limiting arc parameters are not reached in this case, and the values of U, h_c, and the efficiency are higher in a plasmatron with a variable radius than in the case $R=\text{const}$, for equal values of R_1 and G_l. Accordingly, additional improvements in plasmatron properties can be achieved by using channels of appropriate profile and by optimizing the channels in terms of the parameter k. This capability is one of the basic advantages of plasmatrons with arc chambers of variable radius.

These experimental results can be explained and generalized on the basis of the results of [3], where the properties of the positive column of an arc of variable radius were studied. Using the equations of [3] we find an expression for the electric field

$$E=\frac{\mu_1}{R_0\sigma_s^{0.5}(1+kz)}\cdot\frac{I}{\Psi(z,\beta)}, \tag{2}$$

the heat flux,

$$q=\frac{I\Phi'}{R_0\sigma_s^{0.5}\mu_1\gamma_1}\cdot\Psi(z,\beta), \tag{3}$$

the average-mass enthalpy,

$$h_c=h_*+\frac{h_s I}{\pi R_0\sigma_s^{0.5}\mu_1}\cdot\Psi(z,\beta), \tag{4}$$

and the local efficiency of the positive column,

$$\eta=1-\frac{|\Phi'|}{\gamma_1\mu_1^2}(1+kz)\Psi^2(z,\beta). \tag{5}$$

Here

$$\Psi(z,\ \beta) = (1+kz)^{-\frac{\mu_1^2}{\beta}}\left\{\frac{E_0'^2}{E_0^2} + \frac{(1+kz)^{\frac{2\mu_1^2}{\beta}-1}-1}{1-\frac{\beta}{2\mu_1^2}}\right\}^{0.5},$$

$$E_0 = \frac{Ih_s}{\pi R_0\sigma_s(h_{c_*}-h_*)},\quad E_0' = \frac{\mu_1}{R_0\sigma_s^{0.5}},\quad \beta = \frac{kG_0h_s}{\pi L}, \tag{6}$$

μ_1 is the first root of the function $\Phi(\mu,\ r)$ (which describes the profile of the heat-conduction function S along the radius of the positive column),

$$\gamma_1 = \int_0^1 \Phi_1(\mu_1,\ r)\,r\,dr,\quad \Phi_1' = \left[\frac{d\Phi(\mu_1,\ r)}{dr}\right]_{r=1},$$

h_* is the value of h at r = 1, and σ_S and h_S are the derivatives of the electrical conductivity and the enthalpy of the gas with respect to the heat-conduction function. The quantities μ_1, γ_1, and Φ_1' depend on the parameter β; computer-calculated values of these quantities are shown in Table 1.

In Eqs. (3) and (4) the function $\Psi(z, \beta)$ describes the distributions of the relative quantities $(h_c - h_*)\cdot\pi R_0\sigma_S^{0.5}\mu_1/h_S I$ and $qR_0\sigma_S^{0.5}\mu_1\gamma_1/\Phi_1' I$. As we see from (6), the nature of the changes in $\Psi(z, \beta)$ depends on k, i.e., the channel profile, G_0, and E_0. To simplify the analysis of the arc properties we consider only those values of E_0 which correspond to two limiting distributions.

1. $E_0 = E_0'$. In this case the average-mass enthalpy is

$$h_{c_*} = h_* + \frac{h_s I}{\pi R\sigma_s^{0.5}\mu_1};$$

the distributions of η and $\Psi(z, \beta)$ calculated from Eqs. (5) and (6) are shown by curves 1 and 2 in Fig. 3.

2. $E_0 = \infty$. In this case we have $h_{c_0} \simeq h_*$; calculations of η and $\Psi(z, \beta)$ are shown by curves 3 and 4 in Fig. 3. For values of the field in the initial cross section which satisfy the condition $E_0' < E_0 < \infty$, the curves for the distributions of q, h_c, and η lie between the corresponding calculated curves. As E_0 decreases, curves 3 and 4 approach curves 1 and 2, respectively, while cross section Z' shifts toward the origin of coordinates. From (6) we find an equation for Z':

$$Z' = \frac{L}{k}\left\{\left(\frac{kG_0h_s}{2\pi L\mu_1^2\left[1-\frac{E_0'^2}{E_0^2}\left(1-\frac{\beta}{2\mu_1^2}\right)\right]}\right)^{\frac{1}{1-\frac{2\mu_1^2}{\beta}}} - 1\right\}. \tag{7}$$

It follows from Fig. 3 that the form of the distribution $\Psi(z, \beta)$, i.e., the relative values of q and h_c, depends on E_0 only up to cross section Z'; thereafter, q and h_c decrease with increasing z, regardless of the value of E_0. Despite the important changes in E, h_c, and q, the local efficiency η remains nearly independent of z and is quite high, in agreement with the experimental data. This result also speaks in favor of the use of arc chambers of variable radius.

It follows from (3) and the data in Table 1 that in the case of a rapid expansion of the positive column due to a significant gas flow across its surface, the heat loss due to conduction can be reduced essentially to zero. The same effect can occur in a channel of constant radius in the initial part of the arc [9].

Accordingly, the equations of [3] give a qualitatively correct description of these experimental data. The conditions of these experiments (the stepped change in the flow rate, the presence of radial flow, the presence of an electrically insulating gas layer between the arc column and the wall, the radiation, etc.) are quite different from those assumed in [3]. Accordingly, the calculation based on (2)-(7) agrees satisfactorily with experiment only over limited ranges of I, G, and k. However, the equations given here can be used to generalize the experimental data over broad ranges of the parameters.

Figure 4 shows the generalized results for the heat flux at z = 1 and $z = Z_q$ cross sections; curves I and II, respectively, are drawn from the equations

$$q_1 = B_1\left(\frac{I}{\mu_1}\right)^{1.5},\qquad B_1 = 175\,\frac{V\cdot a^{-0.5}}{m\cdot A^{0.5}} \tag{8), (10}$$

$$q_m = B_m\left(\frac{I}{\mu_1}\right)^{1.5}, \qquad B_m = 320\,\frac{V\,a^{-0.5}}{m \cdot A^{0.5}}. \tag{9), (11}$$

Figure 5 shows a generalization of the experimental values of h_c for the plasma at the exit from an arc source, according to Eq. (4). In calculating $\Psi(1, \beta)$ we assumed $E_0 = \infty$ and $h_* = 0.27 \cdot 10^6$ J/kg, corresponding to a temperature of ~300°K. The values of σ_s and h_s for an air plasma were taken from [10].

Accordingly, it has been shown that the use of arc chambers of variable radius can improve the characteristics of plasmatrons. Equations (1)-(11) of this paper, the data in Table 1, and the experimental data can be used to develop plasmatrons of this type.

NOTATION

R, L, radius and length of the arc chamber, m; r, z, coordinates divided by R and L; l_a, l, length of the anode and of the section, m; δ, distance between sections, m; E, electric field, V/m^{-1}; U, arc voltage, V; I, arc current, A: G, mass flow rate of gas, kg/sec^{-1}; G_i, flow rate of the gas flowing between the sections, kg/sec^{-1}; h, enthalpy, J/kg^{-1}; q, heat flux, W/m^{-1}; η, local efficiency of the positive column. Subscripts: c, average-mass value; 0, 1, values at z = 0 and z = 1.

LITERATURE CITED

1. A. I. Zhidovich, S. K. Kravchenko, and O. I. Yas'ko, Inzh.-Fiz. Zh., 15, No. 2 (1968).
2. A. S. An'shakov, G. Yu. Dautov, Yu. S. Dudnikov, I. S. Mazuraitis, and M. I. Sazonov, Fiz. Khim. Obrab. Mater., No. 1 (1969).
3. A. I. Dautov, R. Kh. Ismagilov, and Kh. M. Shavaliev, Inzh.-Fiz. Zh., 25, No. 3 (1973).
4. V. V. Berbasov, V. A. Uryukov, Izv. Sibirsk. Otd. Akad. Nauk SSSR, Ser. Tekh. Nauk, No. 3, Issue 1 (1974).
5. F. S. Abzalova et al., in: Low-Temperature Plasmas, Proceedings of the Kazan' Institute of Aviation [in Russian], Kazan' (1974), No. 165.
6. R. Kh. Ismagilov, Author's Abstract of Candidate's Dissertation, Kazan' (1974).
7. G. M. Mustafin, Zh. Prikl. Mekh. Tekh. Fiz., No. 4 (1968).
8. D. E. Anderson and E. R. Eckert, Raketn. Tekh. Kosmonavt., No. 4 (1967).
9. M. E. Zarudi, in: Modeling and Calculation Methods for Physicochemical Processes in Low-Temperature Plasmas [in Russian], Nauka, Moscow (1974), p. 122.
10. G. Yu. Dautov, in: Sources of Low-Temperature Plasmas [in Russian], Énergiya, Moscow (1969), p. 4.